ADVANCES IN ATMOSPHERIC SCIENCES, VOL. 39, NOVEMBER 2022, 1885–1896

• **Original Paper** •

# Different Impacts of Intraseasonal Oscillations on Precipitation in Southeast China between Early and Late Summers

Junqi LIU[1,2] and Riyu LU[*1,2]

[1]*State Key Laboratory of Numerical Modeling for Atmospheric Sciences and Geophysical Fluid Dynamics, Institute of Atmospheric Physics, Chinese Academy of Sciences, Beijing* 100029, *China*

[2]*College of Earth and Planetary Sciences, University of Chinese Academy of Sciences, Beijing* 100029, *China*

(Received 31 August 2021; revised 8 February 2022; accepted 11 February 2022)

ABSTRACT

This study investigates the influences of boreal summer intraseasonal oscillation (BSISO), which originates from the equatorial Indian Ocean and prevails over the Indo-Pacific region, on precipitation over Southeast China, including South China and Yangtze River Valley. The results indicate that the BSISO-related precipitation anomalies are remarkably different between early summer (May–June) and late summer (July–August). The BSISO-related precipitation anomalies tend to appear more northward in late summer in comparison with early summer. Accordingly, the BSISO is significantly related to precipitation anomalies over South China during many phases in early summer but related to very weak anomalies during all the phases in late summer. Such northward shifts of precipitation anomalies from early summer to late summer are clearest during phases 4 and 7, when the lower-tropospheric anticyclonic and cyclonic circulation anomalies dominate over the subtropical western North Pacific, respectively. Finally, we explain the differences between early and late summers through the seasonal northward migration of climatological equivalent potential temperature gradient, which is located in the South China during early summer but migrates northward to the YRV during late summer.

**Key words:** intraseasonal oscillation, precipitation, Southeast China

**Citation:** Liu, J. Q., and R. Y. Lu, 2022: Different impacts of intraseasonal oscillations on precipitation in Southeast China between early and late summers. *Adv. Atmos. Sci.*, **39**(11), 1885−1896, https://doi.org/10.1007/s00376-022-1347-4.

**Article Highlights:**

- The BSISO-related precipitation anomalies tend to appear more northward in late summer in comparison with early summer.
- The BSISO corresponds significantly to the precipitation anomalies over the South China in early summer but very weak anomalies in late summer.
- The remarkable difference is attributed to the northward shifts of climatological equivalent potential temperature gradient from early to late summer.

## 1. Introduction

Southeast China (SEC), including the South China (SC) and the Yangtze River Valley (YRV), is a densely populated area and one of the most important economic centers in China. The summer precipitation over SEC is closely related to the East Asian summer monsoon and shows a significant intraseasonal variability (e.g., Mao and Wu, 2006; Mao et al., 2010; Yang et al., 2010; Sun et al., 2016). The strong precipitation variability often triggers floods and thus leads to disasters to the economy and society in SEC. For instance, a heavy rainfall in SC caused 168 people dead and destroyed 45600 houses during early summer of 2008 (Wang et al., 2011), and the heavy flooding in the YRV during the summer of 1998 caused 3000 deaths and 260 billion China Yuan of economic losses (Huang et al., 1998). Therefore, investigating the intraseasonal variability in summer precipitation over SEC is of great significance.

The intraseasonal oscillations in the tropics are the major predictability source for subseasonal-to-seasonal prediction not only in the tropics but also in many extratropical regions (Webster et al., 1998; Waliser et al., 2003; Vitart et al., 2017). The boreal summer intraseasonal oscillation (BSISO) propagates northward or northeastward over the tropical Indian Ocean (Yasunari, 1979, 1980; Jiang et al., 2004; Li, 2014) and northward or northwestward over the tropical western North Pacific (WNP) (Murakami, 1980; Chen and

* Corresponding author: Riyu LU
Email: lr@mail.iap.ac.cn

Chen, 1995; Wang et al., 2018b). In order to describe BSISO, Lee et al. (2013) defined the BSISO real-time indices through multivariate empirical orthogonal function (MV-EOF) analysis of the daily anomalies of outgoing longwave radiation (OLR) and zonal wind at 850 hPa over the Asian summer monsoon region. Two kinds of BSISO can be identified accordingly, i.e., BSISO1 and BSISO2. The BSISO1 represents the canonical northward/northeastward propagating oscillations with period of 30–60 days, and BSISO2 capture the northwestward propagating oscillations with period of 10–20 days (Chen and Chen, 1995; Annamalai and Slingo, 2001; Annamalai and Sperber, 2005; Wang et al., 2018b). Previous studies suggested that BSISO1 exhibits a high potential predictability (e.g., Lee et al., 2015; Wang et al., 2019). Therefore, the influence of BSISO1 on SEC precipitation may help us better understand the potential predictability of precipitation variations over SEC on the intraseasonal timescale. In this study, the influences of BSISO1 on precipitation over SEC are focused on, and thus the BSISO1 is highlighted in the following. Hereafter, BSISO1 is referred to as BSISO.

Previous studies have shown that the BSISO, or 30–60-day oscillation, has a clear influence on summer precipitation over SEC. It was found that the BSISO-related convection anomalies over the WNP can cause the westward extension or eastward retreat of the western North Pacific subtropical high (WNPSH), thus affecting the summer precipitation over SEC (Zhu et al., 2003; Mao et al., 2010). In addition, convection anomalies over the tropical Indian Ocean also affect the summer precipitation over SEC by generating northeastward propagating Rossby waves from the tropical Indian Ocean to East Asia or coupling with the convection over the WNP (Zhang et al., 2009; Li et al., 2015; Sun et al., 2016).

It has been well known that the mean state, including atmospheric circulation and rainfall, shows a pronounced seasonal evolution over the WNP and East Asia (Lau et al., 1988; Wang et al., 2009). First, the WNPSH advances northward and retreats eastward in late summer in comparison with early summer (e.g., Lu, 2001; Su et al., 2014; Yuan et al., 2019). Additionally, the westerly jet in the upper troposphere shifts northward significantly from early to late summer (e.g., Lin and Lu, 2008; Sampe and Xie, 2010; Chiang et al., 2017; Wang et al., 2018a). Corresponding to these circulation changes, the major rainy region shifts from SC to the north of the Yangtze River (e.g., Tao and Chen, 1987; Ding and Chan, 2005).

These seasonal changes in climatological condition may result in different relationships between tropical and extratropical anomalies. Using idealized numerical experiments, Kosaka and Nakamura (2010) showed that identical tropical forcing can trigger northward extended circulation responses in the subtropics called the Pacific-Japan pattern in the situation of a northward shifted climatological westerly jet and meridional extension of WNPSH. In addition, seasonal changes in the tropical-extratropical relationship can also be found. For instance, Lu (2004) showed that the meridional teleconnections are stronger in July and August over the WNP and East Asia, in comparison with June. Wang et al. (2009) indicated that the spatial distribution of El Niño–Southern Oscillation-related precipitation is different over East Asia from May–June to July–August. Li and Lu (2018) suggested that the convection over WNP exerts different influences on precipitation in the YRV during the different stages of summer due to the seasonal evolution of climatological general circulation in East Asia. Furthermore, Liu et al. (2020) suggested that the intraseasonal variability of China summer precipitation features a distinct three-stage evolution during summer, and it has a distinct relationship with the mid-latitude wave train and tropical intraseasonal oscillation in the different stages of summer. Therefore, a question naturally arises: Does the BSISO, which can be considered as tropical forcing, induce different influence on precipitation over SEC between early and late summer? This is the main motivation of this study.

In this study, we investigated the differences in the influence of the BSISO on precipitation over SEC between early and late summer. The remainder of this paper is organized as follows. Section 2 describes the datasets and methods used in this study. Section 3 presents the impact of BSISO on precipitation over the SEC during MJ and JA. Section 4 presents the circulation anomalies related to BSISO during MJ and JA. Finally, the conclusions and discussion are offered in section 5.

## 2. Data and analysis methods

In this study, we defined SEC as the land area in mainland China east of 105°E and between 20°N and 35°N. The southern rectangle in Fig. 1 represents the SC (20°–28°N) and the northern rectangle represents the YRV (28°–35°N). The early summer and late summer are simply denoted as May–June (MJ) and July–August (JA), respectively, which can represent the major features of seasonal evolution over the WNP and East Asia. We used 20 June and 10 July as the partition dates; the results suggest that our conclusions are not sensitive to the partition method of early and late summer. Figure 1 also shows the notable seasonal march of the climatological mean precipitation from MJ to JA. As mentioned in the introduction, the major rainy regions are located over SEC in MJ, and march northward to north of the Yangtze River in JA.

The precipitation data used in this study are the CN05.1 dataset (Wu and Gao, 2013) from the National Climate Center in China. The dataset is gridded data based on 2400 stations in China (their Fig. 1). These stations are densely spaced and evenly distributed throughout Eastern China, which is the interest region of this study. In addition, the European Centre for Medium-Range Weather Forecasts (ECMWF) daily reanalysis dataset (ERA5; Hersbach et al., 2020), including horizontal wind, geopotential height ($Z$), specific humidity and air temperature, is also used. Finally, the daily outgo-

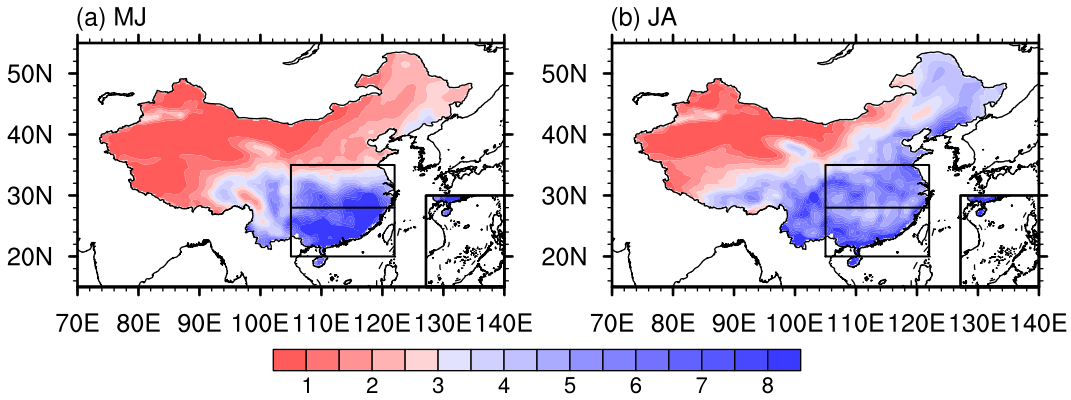


**Fig. 1.** (a) May–June (MJ) and (b) July–August (JA) climatologies of precipitation (mm $d^{-1}$) in China from 1981 to 2018. The southern (20°–28°N) and northern (28°–35°N) rectangles represent the SC and YRV regions, respectively.

ing longwave radiation (OLR) data from the National Oceanic and Atmospheric Administration (NOAA) are used as a proxy for tropical convective activity. The horizontal resolution is 0.25° × 0.25° for the CN05.1, and 2.5° × 2.5° for the ERA5 dataset and OLR data. All these data from 1981 to 2018 were used for the analyses of this study.

The BSISO is identified according to the approach of Lee et al. (2013), who developed real-time multivariate indices for BSISO. The BSISO indices represent fractional variance and the observed northward propagating ISO over the Asian summer monsoon region. The indices are obtained by using MV-EOF analysis of daily mean OLR and 850-hPa zonal wind anomalies over the Asia summer monsoon region (10°S–40°N, 40°–160°E). BSISO is defined by the 1st and 2nd principal components (PC1 and PC2) of MV-EOF. The BSISO indices represent the canonical northward propagating BSISO with the period of 30–60 days. Similar to the real-time multivariate MJO index (Wheeler and Hendon, 2004), BSISO can be divided into 8 phases, and an active BSISO event is defined as $(PC1^2 + PC2^2)^{1/2} > 1$. Therefore, in general, only a few days are selected for composite analyses in each phase. The BSISO indices are obtained online at https://apcc21.org/ser/moni.do?lang=en.

Following Lee et al. (2013), the anomalies of variables are calculated by removing the mean values and the first three harmonics of multi-year averages, which are considered as the annual cycle. The statistical significance is examined by the two-tailed Student's *t* test. The effective degrees of freedom are estimated as follows (Zwiers and von Storch, 1995): the effective degrees of freedom is Ne = $N[(1–r1)/(1+r1)]$, where $N$ is the sample size of total days and r1 is the lag-one autocorrelation; then, if r1 is significant at the 95% confidence level using Ne, the effective degrees of freedom is Ne, otherwise it is $N$.

## 3. Influence of the BSISO on precipitation in Southeast China

Figure 2 depicts the precipitation anomalies during the active phases of BSISO in MJJA. The BSISO-related precipitation anomalies over the SEC are generally positive during phases 2–4 and negative during phases 5–7. The most significant anomalies appear during phase 7, when the anomalies are negative over almost the entirety of SEC. In contrast, positive anomalies appear over most of SEC during phase 4, but they group into two bands over the SC and YRV, respectively. These BSISO-related precipitation anomalies are in good agreement with the results of precipitation extremes related to BSISO during May–August (Hsu et al., 2016; Chen and Zhai, 2017), which suggests a close relationship between mean precipitation and precipitation extremes.

Figure 3 shows the regional mean precipitation anomalies over the SC and YRV during the active phases of BSISO in MJJA. The SC precipitation anomalies are significantly positive during phase 4 and negative during phases 5–7, being 1.3 and –1.0 mm $d^{-1}$, respectively. These anomalies are equivalent to 17.8% and 13.7% of the climatological mean over the SC (7.3 mm $d^{-1}$), suggesting a great influence of BSISO. In addition, the precipitation anomalies over the YRV are significantly positive during phases 2–4 and negative during phases 6–8. The precipitation anomalies averaged over these phases are 1.1 and –0.9 mm $d^{-1}$, which are equivalent to 20.7% and 17.0% of the climatological mean in the YRV (5.3 mm $d^{-1}$), respectively.

Figure 4 shows the precipitation anomalies during the active phases of BSISO in MJ and JA. The precipitation anomalies are positive during phases 2–4 and negative during phase 5–7 in MJ. During most phases, the precipitation anomalies tend to be stronger over the SC region. It can also be seen that the positive precipitation anomalies are located in the YRV in phase 2, which are more northward than those in phase 4. This issue will be discussed further in the next section.

The precipitation anomalies in JA are in sharp contrast with those for MJ. For instance, during phase 4, the positive precipitation anomalies are concentrated in the YRV in JA (Fig. 4b), whereas they are mainly located in the SC region in MJ (Fig. 4a). Additionally, the negative anomalies are considerably weakened during phases 5–7 in JA, particularly

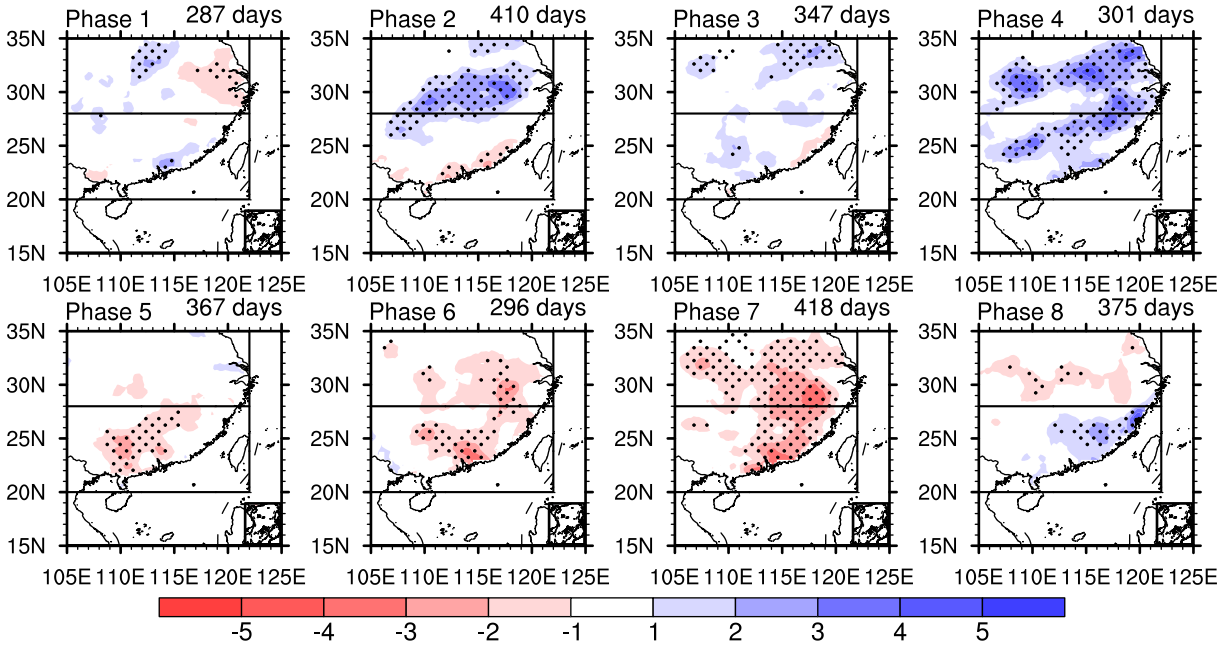


**Fig. 2.** Precipitation anomalies (shading, mm $d^{-1}$) during the 8 active phases of the BSISO in MJJA. Black dots denote the precipitation anomalies that pass the 95% confidence level based on the Student's *t* test.

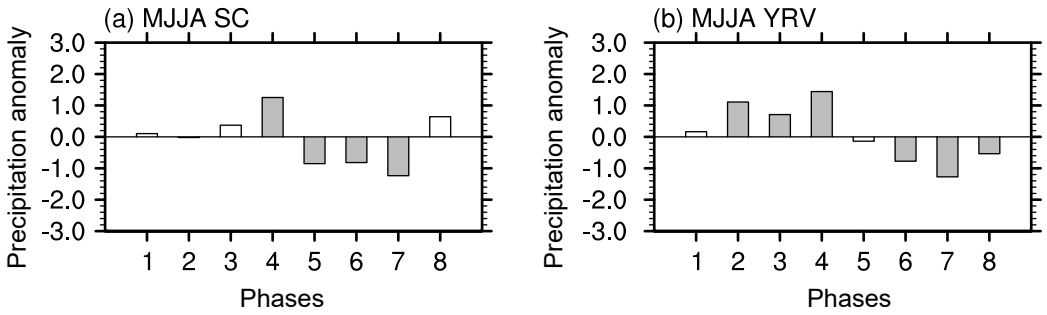


**Fig. 3.** Composite regional mean precipitation anomalies (mm $d^{-1}$) over (a) SC and (b) YRV during active phases of the BSISO in MJJA. The shading bars denote the precipitation anomalies at the 95% confidence level.

over the SC region. These differences between MJ and JA demonstrate that it is reasonable and necessary to distinguish early from late summer when the impacts of BSISO on precipitation over the SEC are discussed. We repeated this figure by using station precipitation data from the Chinese Meteorological Administration and using the CPC global precipitation dataset (figures not shown) and found that the results are consistent with Fig. 4, suggesting that the results on precipitation anomalies are robust.

Figure 5 shows the regional mean precipitation anomalies over the SC and YRV during the active phases of BSISO in MJ and JA. In MJ, the BSISO has significant impacts on precipitation over the SC (Fig. 5a). The maximum positive and negative precipitation anomalies appear during phase 4 and phase 7 and are 2.5 and –2.0 mm $d^{-1}$, which are equivalent to 30.1% and 24.1% of the climatological mean (8.3 mm $d^{-1}$), respectively. The SC precipitation anomalies are much weakened and not significant in all the phases of BSISO in JA (Fig. 5c). On the other hand, the YRV precipitation anomalies seem not to show such a sharp difference between early and late summer (Figs. 5b and 5d), being positive during phases 2–4 and negative during phases 6–8 for both early and late summers. However, as shown in Figs. 4, there are indeed considerable differences in the distributions of precipitation anomalies between early and late summer. For instance, the significant anomalies during both phases 4 and 7 appear at the southern part of the SEC in MJ but shift northward to the northern part of the SEC in JA. Therefore, the somewhat vague differences shown in Figs. 5b and 5d may be due to the overlapped anomalies over the YRV between MJ and JA. In JA, phases 4 and 7 are also characterized by the strongest anomalies over the YRV (Fig. 5d). The YRV anomalies are 2.1 and –1.3 mm $d^{-1}$ during phase 4 and phase 7, which are equivalent to 38.2% and 23.6% of the climatological mean (5.5 mm $d^{-1}$), respectively.

It should be noted that the precipitation anomalies exhibit some clear asymmetries. For instance, in MJ the anomalies over South China are significantly negative during

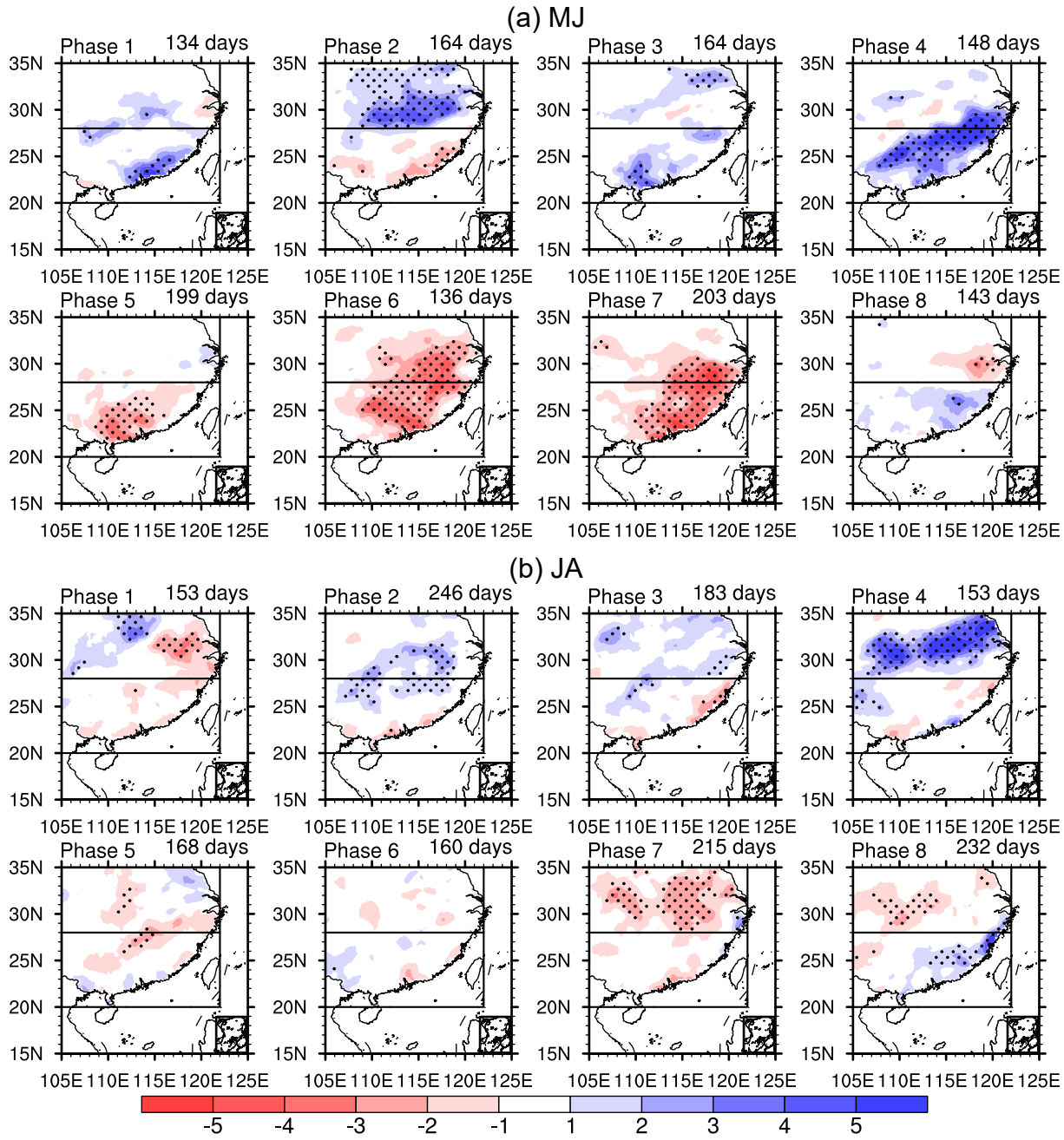


**Fig. 4.** As in Fig. 2 but for MJ and JA.

phases 5–7 but significantly positive only during phase 4 and even negative during phase 2 (Fig. 5a). These asymmetries might be due to the fact that precipitation is a variable of great variability on both the temporal and spatial scales, and thus the results on precipitation are highly sensitive to the sample size.

## 4. Circulation anomalies related to BSISO during early and late summers

In this section, we examine the circulation anomalies associated with BSISO in MJ and JA, in an attempt to explain the distinct impacts of BSISO on precipitation in the SEC region between these two periods. To facilitate the comparison with convection, which is also an element for the BSISO definition in addition to 850-hPa zonal wind, OLR anomalies associated with BSISO are also shown.

Figure 6 depicts the OLR and horizontal wind anomalies at 850 hPa during the active phases of BSISO in MJ and JA. As well documented in previous studies (e.g., Lee et al., 2013; Ren et al., 2018), the BSISO-related convection propagates generally northeastward. The negative OLR anomalies propagate from the equatorial Indian Ocean to the Bay of Bengal from phase 1 to phase 4, and the positive anomalies propagate over the similar route from phase 5 to phase 8. Over the WNP, the anomalous convection tends to propagate north-

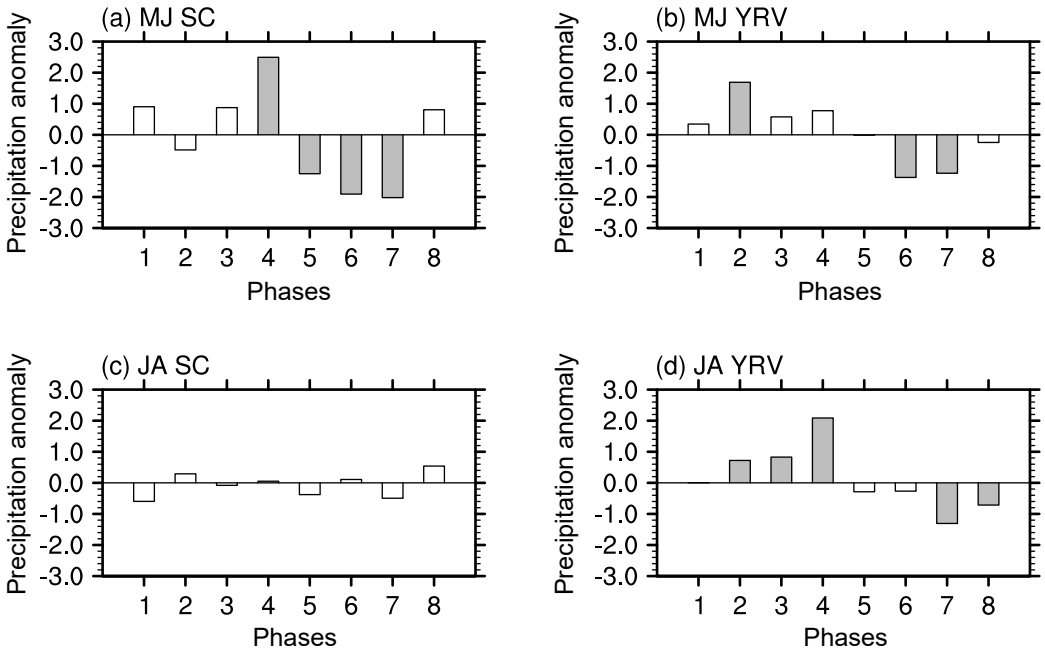


**Fig. 5.** Composites of the regional mean precipitation anomalies (mm $d^{-1}$) in the SC (a, c) and YRV (b, d) during active phases of the BSISO in MJ (a, b) and JA (c, d). The shading bars denote the precipitation anomalies at the 95% confidence level.

ward. For instance, during phases 4–8, the enhanced convection propagates northward from the Maritime Continent to the subtropical WNP.

During phases 1–4, there is an anomalous anticyclone over the South China Sea and WNP. The anomalous anticyclone appears over the South China Sea and Bay of Bengal during phase 1, propagates northeastward during subsequent phases, and appears over the subtropical WNP during phase 4. This anomalous anticyclone is associated with suppressed convection, i.e., positive OLR anomalies to its south, which also propagate from the Bay of Bengal and South China Sea to the subtropical WNP. During phases 5–8, the OLR and horizontal wind anomalies show a mirror pattern. In addition, the anticyclonic anomalies are similar between phase 2 and phase 4, and thus it is surprising that the precipitation anomalies are so different between these phases (Fig. 4). We speculate that the unstable distribution of precipitation may be due to the insufficient sample size. Precipitation is a variable of great variability for both temporal and spatial scales, and thus might be highly sensitive to the sample size.

The BSISO-related wind anomalies in JA (Fig. 6b) are like those in MJ, i.e., there is also anomalous anticyclone during phases 1–4 and cyclone during phases 5–8 over the South China Sea and WNP. These wind anomalies can generally explain the precipitation anomalies associated with BSISO shown in the preceding section, i.e., the anomalous anticyclone favors more water vapor transport into the SEC region and heavier rainfall there during phases 1–4, while the anomalous cyclone play an opposite role during phases 5–8.

We have also examined the circulation anomalies at 200 hPa in MJ and JA (figures not shown), considering that the upper-tropospheric circulation anomalies may also be related to the BSISO (Jiang et al., 2004; Chen et al., 2015), and found that the wind anomalies are not well organized in southeastern China and the subtropical WNP. Therefore, in this study we focus on the BSISO-related wind anomalies in the lower troposphere.

The column-integrated moisture flux and its divergence are shown in Fig. 7 to further investigate the northward shift in precipitation areas. For simplicity, we only show the moisture transport composites in phases 4 and 7. These two phases are also characterized by distinct precipitation anomalies between early and late summer, as shown in the preceding section. The column-integrated moisture flux divergence correlates well to the precipitation anomalies. In MJ, the moisture flux is primarily convergent over the SC region during phase 4. In contrast to MJ, the convergence region of moisture flux is mainly located in the YRV region during phase 4 in JA. The moisture transports during phase 7 are opposite to those during phase 4.

These results suggest that the BSISO-related precipitation anomalies are quite distinct between MJ and JA, although the circulation anomalies are similar. In the following, we attempt to explain this through analyzing the equivalent potential temperature, which includes both temperature and humidity, and is widely used to illustrate the formation of summer precipitation over the SEC (e.g., Chen and Zhai, 2015; Park et al., 2015; Li and Lu, 2018). It is well known that the strong meridional gradient of equivalent potential temperature, in association with the southern warm and moist airmass, is favorable for precipitation over the SEC during summer.

Figure 8 shows the climatological equivalent potential

temperature in MJ and JA at 850 hPa. In MJ, the warm and moist airmass is located over the northern Indochina Peninsula. The strong meridional gradient of climatological equivalent potential temperatures appears over SC, which corresponds well to the heavy rainfall there. The meridional gradient is also strong over the YRV region, but it seems to be more attributed to the cold and dry airmass in the extratropics. On the other hand, in JA, the warm, moist airmass extends considerably northward, and the strong meridional gradient shifts northward to the YRV, and thus the similar southerly anomalies lead to rainfall enhancement in the YRV in JA. Therefore, the distinct horizontal distributions of climatological equivalent potential temperature can help to explain the different distributions of precipitation anomalies between MJ and JA. In addition, the stronger southwesterly anomalies during phase 4 over the SEC in JA compared to MJ might lead to stronger moisture transport to the YRV (Figs. 6 and 7) and be another factor that causes the northward shift of precipitation anomalies.

## 5. Summary

In this study, we studied the influences of BSISO on precipitation over Southeast China (SEC), including South

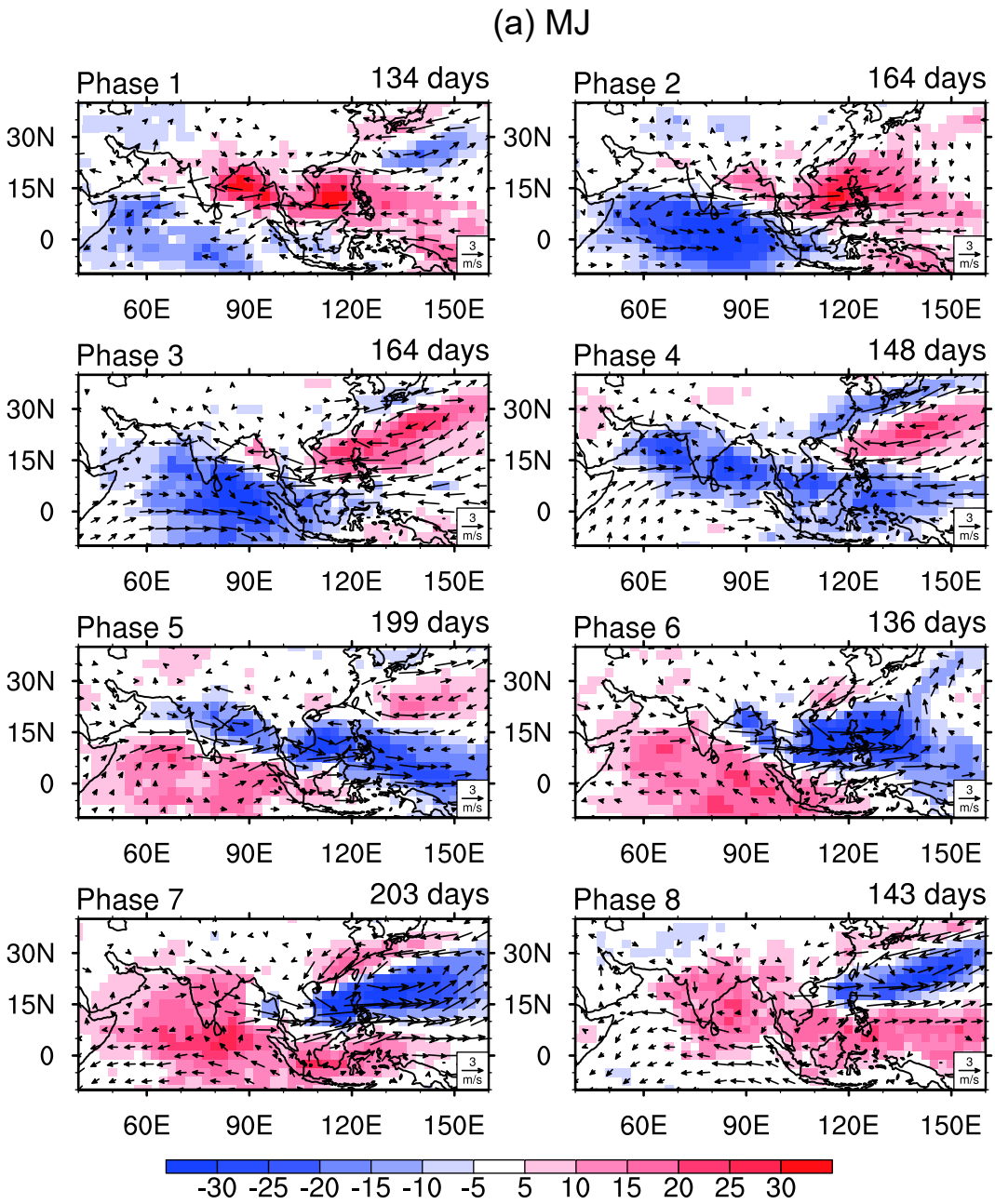


**Fig. 6.** Composites of OLR (shading, W $m^{-2}$) and horizontal wind (vector, m $s^{-1}$) anomalies at 850 hPa during active phases of the BSISO in MJ and JA. Only anomalies significant at the 95% confidence level are shown.

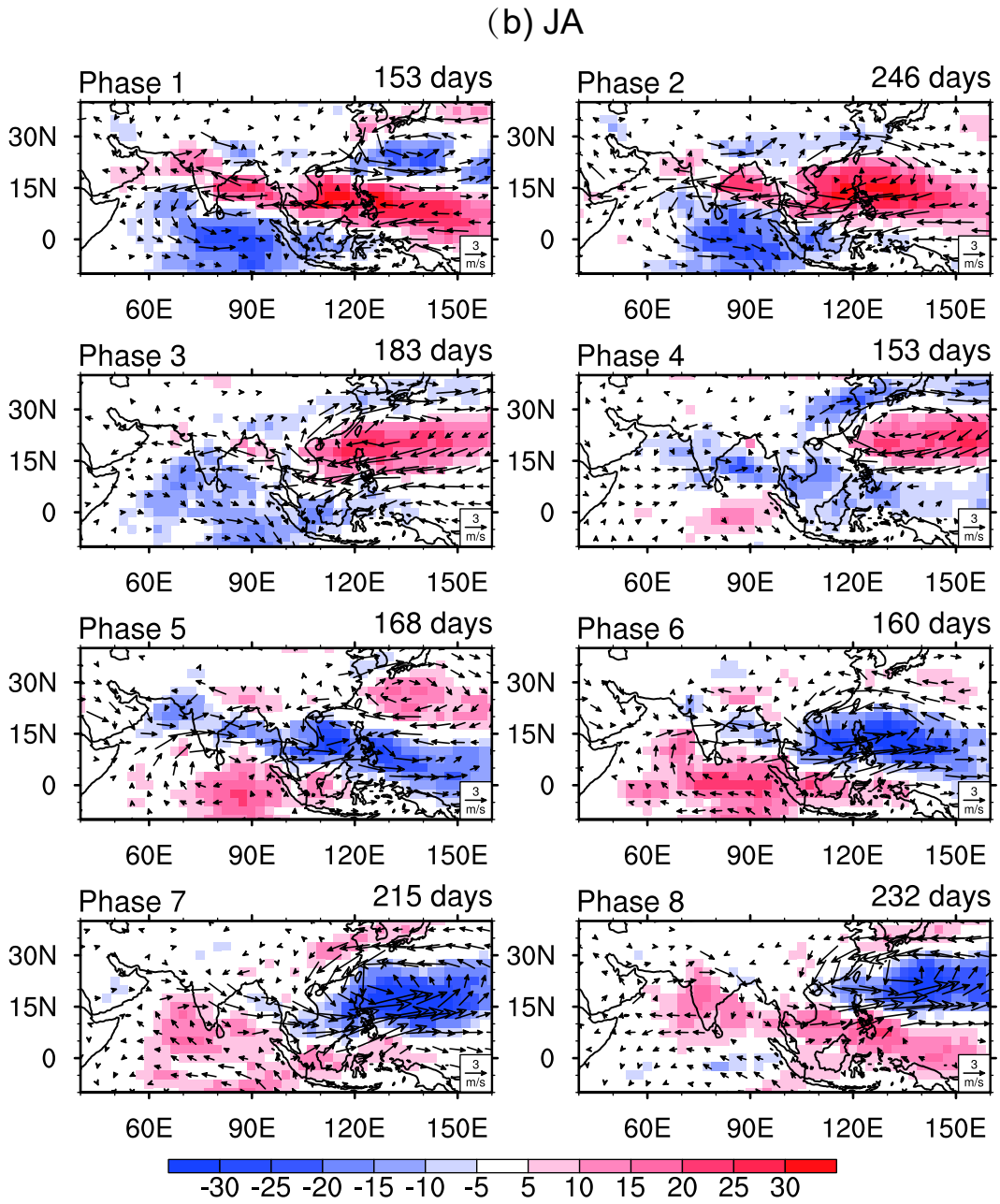


**Fig. 6.** (Continued).

China (SC) and the Yangtze River Valley (YRV), during early summer (May–June, MJ) and late summer (July–August, JA). The BSISO-related precipitation anomalies are generally positive during phases 2–4 and negative during phases 5–7 over the SEC in the entire summer (May–August). However, the BSISO-related precipitation anomalies are considerably different between MJ and JA. The most remarkable difference is manifested over SC: the BSISO is significantly related to precipitation anomalies over this region during phases 4–7 in MJ, but absolutely not in JA. For instance, in MJ the precipitation anomalies averaged over SC are 2.5 and –2.0 mm $d^{-1}$ during phases 4 and 7, respectively, equivalent to 30.1% and 24.1% of the climatological mean. By contrast, in JA the precipitation anomalies averaged over SC are very weak, lower than 0.6 mm $d^{-1}$ during all the active phases. The other notable difference is the northward shift of BSISO-related precipitation anomalies: the significant precipitation anomalies are concentrated over SC or to the south of the Yangtze River in MJ, but they shift to the north of the river in JA, during both phases 4 and 7. These important differences between MJ and JA suggest that it is necessary to separate early and late summer periods for better understanding the impacts of BSISO on rainfall in the SEC area.

The lower-tropospheric circulation anomalies, which are crucial for water vapor transport over the SEC, were exam-

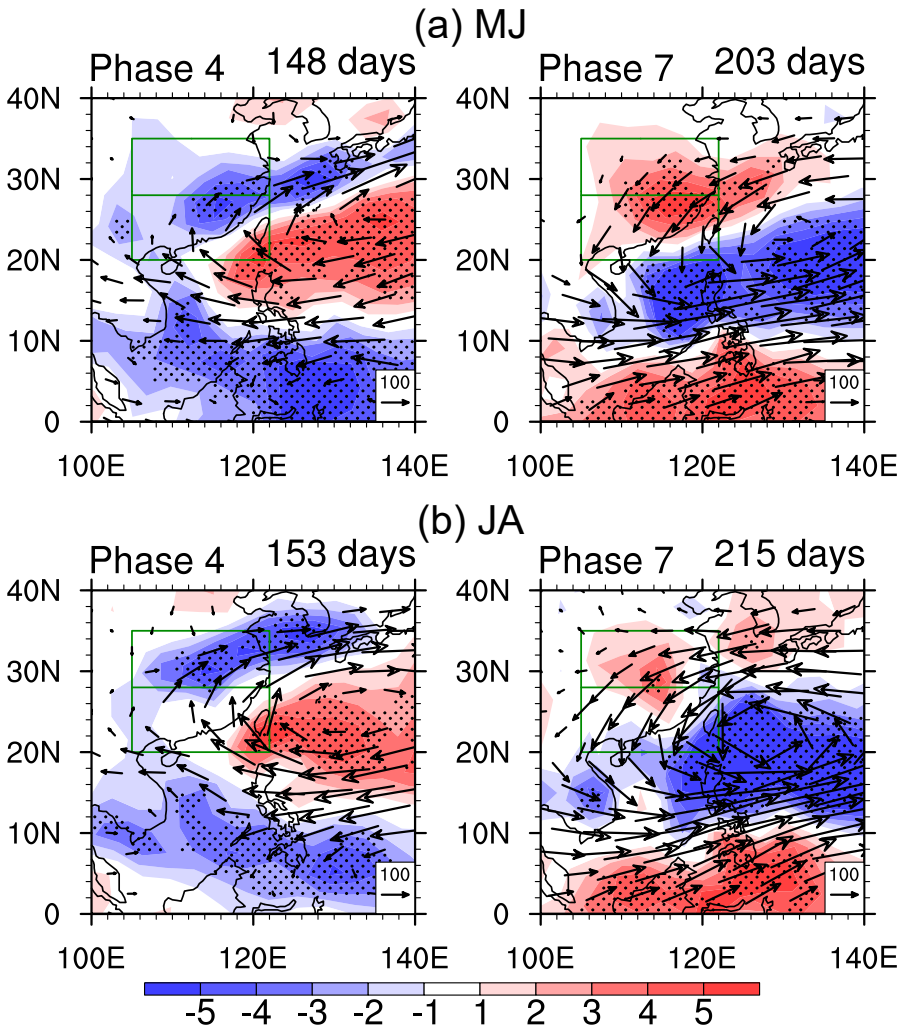


**Fig. 7.** Composites of the column-integrated moisture flux (vector, kg $m^{-1}$ $s^{-1}$) and its divergence (shading, mm $d^{-1}$) anomalies during phase 4 and phase 7 in MJ (a) and JA (b). Black dots denote the moisture flux divergence anomalies that pass the 95% confidence level.

ined to explain the distinct impacts of BSISO on precipitation between MJ and JA. Generally, the significant positive and negative precipitation anomalies over the SEC area are related to the anomalous anticyclones and cyclones over the South China Sea and WNP, respectively. The anomalous anticyclone/cyclone could enhance/suppress moisture transport and cause moisture convergence/divergence over the SEC.

Although the anomalous anticyclone and cyclone are similar between MJ and JA, the distributions of BSISO-related precipitation anomalies are extraordinarily different. We suggested that the different precipitation anomalies over SEC may be due to the seasonal change of climatological equivalent potential temperature. In MJ, the meridional gradient of climatological equivalent potential temperatures is strong over the SC region and indicates that the boundary between the tropical warm and moist airmass and extratropical cold and dry airmass appear over SC. However, in JA, the strong meridional gradient of climatological equivalent potential temperatures is located in the YRV, corresponding to the seasonal northward migration of the warm and moist airmass. Therefore, the similar circulation anomalies related to BSISO induce different precipitation anomalies over the SEC between MJ and JA.

Considering that the air-sea interaction may play a role in BSISO (e.g., Kemball-Cook and Wang, 2001; Wang et al., 2018b; Gao et al., 2019), we also composited the BSISO-related SST anomalies using the same method of Fig. 6 (figure not shown). The SST and OLR anomalies are generally in phase over the WNP. Therefore, these SST anomalies may be attributed to the radiation process which is caused by the BSISO circulation anomalies.

In addition, this study focuses on the impacts of BSISO, which originates in the tropics. However, various studies have indicated that the circulation anomalies in the mid and high latitudes can affect rainfall or rainfall extremes in SEC (e.g., Li and Mao, 2019; Liu et al., 2020). These extratropical circulation anomalies may result in the unstable patterns of rainfall anomalies during some phases (for instance, phases 2 and 3). Therefore, the influences of extratropical anomalies on the SEC precipitation during early and late summer need

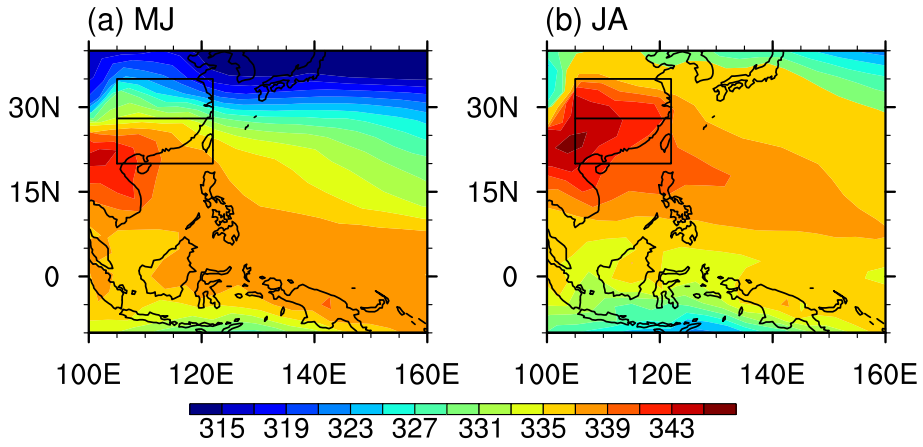


**Fig. 8.** Climatological 850-hPa equivalent potential temperature (shading, K) in (a) MJ and (b) JA.

to be studied in the future.

***Acknowledgements***. The authors highly appreciate the reviewers for their constructive comments, which were most helpful for modulating the discussion on physical mechanism and improving the presentation. This work was supported by the National Natural Science Foundation of China (Grant No. 41721004).

## REFERENCES

Annamalai, H., and J. M. Slingo, 2001: Active/break cycles: Diagnosis of the intraseasonal variability of the Asian summer monsoon. *Climate Dyn.*, **18**, 85–102, https://doi.org/10.1007/s003820100161.

Annamalai, H., and K. R. Sperber, 2005: Regional heat sources and the active and break phases of boreal summer intraseasonal (30–50 day) variability. *J. Atmos. Sci.*, **62**, 2726–2748, https://doi.org/10.1175/JAS3504.1.

Chen, J., Z. Wen, R. Wu, and Z. Chen, 2015: Influences of northward propagating 25–90-day and quasi-biweekly oscillations on Eastern China summer rainfall. *Climate Dyn.*, **45**, 105–124, https://doi.org/10.1007/s00382-014-2334-y.

Chen, Y., and P. M. Zhai, 2015: Synoptic-scale precursors of the East Asia/Pacific teleconnection pattern responsible for persistent extreme precipitation in the Yangtze River valley. *Quart. J. Roy. Meteor. Soc.*, **141**, 1389–1403, https://doi.org/10.1002/qj.2448.

Chen, Y., and P. M. Zhai, 2017: Simultaneous modulations of precipitation and temperature extremes in southern parts of China by the boreal summer intraseasonal oscillation. *Climate Dyn.*, **49**, 3363–3381, https://doi.org/10.1007/s00382-016-3518-4.

Chen, T.-C., and J.-M. Chen, 1995: An observational study of the South China Sea monsoon during the 1979 summer: Onset and life cycle. *Mon. Wea. Rev.*, **123**, 2295–2318, https://doi.org/10.1175/1520-0493(1995)123<2295:AOSOTS>2.0.CO;2.

Chiang, J. C. H., L. M. Swenson, and W. Kong, 2017: Role of seasonal transitions and the westerlies in the interannual variability of the East Asian summer monsoon precipitation. *Geophys. Res. Lett.*, **44**, 3788–3795, https://doi.org/10.1002/2017GL072739.

Ding, Y., and J. C. L. Chan, 2005: The East Asian summer monsoon: An overview. *Meteorol. Atmos. Phys.*, **89**, 117–142, https://doi.org/10.1007/s00703-005-0125-z.

Gao, Y. X., N. P. Klingaman, C. A. DeMott, and P.-C. Hsu, 2019: Diagnosing ocean feedbacks to the BSISO: SST-modulated surface fluxes and the moist static energy budget. *J. Geophys. Res.*, **124**, 146–170, https://doi.org/10.1029/2018JD029303.

Hersbach, H., and Coauthors, 2020: The ERA5 global reanalysis. *Quart. J. Roy. Meteor. Soc.*, **146**, 1999–2049, https://doi.org/10.1002/qj.3803.

Hsu, P.-C., J.-Y. Lee, and K.-J. Ha, 2016: Influence of boreal summer intraseasonal oscillation on rainfall extremes in southern China. *International Journal of Climatology*, **36**, 1403–1412, https://doi.org/10.1002/joc.4433.

Huang, R. H., Y. H. Xu, P. F. Wang, and L. T. Zhou, 1998: The features of the catastrophic flood over the Changjiang River basin during the summer of 1998 and cause exploration. *Climatic and Environmental Research*, **3**, 300–313, https://doi.org/10.3878/j.issn.1006-9585.1998.04.02. (in Chinese with English abstract)

Jiang, X. A., T. Li, and B. Wang, 2004: Structures and mechanisms of the northward propagating boreal summer intraseasonal oscillation. *J. Climate*, **17**, 1022–1039, https://doi.org/10.1175/1520-0442(2004)017<1022:SAMOTN>2.0.CO;2.

Kemball-Cook, S., and B. Wang, 2001: Equatorial waves and air-sea interaction in the boreal summer intraseasonal oscillation. *J. Climate*, **14**, 2923–2942, https://doi.org/10.1175/1520-0442(2001)014<2923:EWAASI>2.0.CO;2.

Kosaka, Y., and H. Nakamura, 2010: Mechanisms of meridional teleconnection observed between a summer monsoon system and a subtropical anticyclone. Part I: The Pacific-Japan pattern. *J. Climate*, **23**, 5085–5108, https://doi.org/10.1175/2010JCLI3413.1.

Lau, K.-M., G. J. Yang, and S. H. Shen, 1988: Seasonal and intraseasonal climatology of summer monsoon rainfall over East Asia. *Mon. Wea. Rev.*, **116**, 18–37, https://doi.org/10.1175/1520-0493(1988)116<0018:SAICOS>2.0.CO;2.

Lee, J.-Y., B. Wang, M. C. Wheeler, X. H. Fu, D. E. Waliser, and I.-S. Kang, 2013: Real-time multivariate indices for the boreal summer intraseasonal oscillation over the Asian summer monsoon region. *Climate Dyn.*, **40**, 493–509, https://doi.org/10.1007/s00382-012-1544-4.

Lee, S. S., B. Wang, D. E. Waliser, J. M. Neena, and J.-Y. Lee, 2015: Predictability and prediction skill of the boreal summer intraseasonal oscillation in the Intraseasonal Variability Hindcast Experiment. *Climate Dyn.*, **45**, 2123–2135, https://doi.org/10.1007/s00382-014-2461-5.

Li, J. Y., and J. Y. Mao, 2019: Coordinated influences of the tropical and extratropical intraseasonal oscillations on the 10–30-day variability of the summer rainfall over southeastern China. *Climate Dyn.*, **53**, 137–153, https://doi.org/10.1007/s00382-018-4574-8.

Li, J. Y., J. Y. Mao, and G. X. Wu, 2015: A case study of the impact of boreal summer intraseasonal oscillations on Yangtze rainfall. *Climate Dyn.*, **44**, 2683–2702, https://doi.org/10.1007/s00382-014-2425-9.

Li, T., 2014: Recent advance in understanding the dynamics of the Madden-Julian oscillation. *Journal of Meteorological Research*, **28**, 1–33, https://doi.org/10.1007/s13351-014-3087-6.

Li, X. Y., and R. Y. Lu, 2018: Subseasonal change in the seesaw pattern of precipitation between the Yangtze River basin and the tropical western North Pacific during Summer. *Adv. Atmos. Sci.*, **35**, 1231–1242, https://doi.org/10.1007/s00376-018-7304-6.

Lin, Z. D., and R. Y. Lu, 2008: Abrupt northward jump of the East Asian upper-tropospheric jet stream in mid-summer. *J. Meteor. Soc. Japan*, **86**, 857–866, https://doi.org/10.2151/jmsj.86.857.

Liu, F., Y. Ouyang, B. Wang, J. Yang, and P.-C. Hsu, 2020: Seasonal evolution of the intraseasonal variability of China summer precipitation. *Climate Dyn.*, **54**, 4641–4655, https://doi.org/10.1007/s00382-020-05251-0.

Lu, R. Y., 2001: Interannual variability of the summertime North Pacific subtropical high and its relation to atmospheric convection over the warm pool. *J. Meteor. Soc. Japan*, **79**, 771–783, https://doi.org/10.2151/jmsj.79.771.

Lu, R. Y., 2004: Associations among the components of the East Asian summer monsoon system in the meridional direction. *J. Meteor. Soc. Japan*, **82**, 155–165, https://doi.org/10.2151/jmsj.82.155.

Mao, J. Y., and G. X. Wu, 2006: Intraseasonal variations of the Yangtze rainfall and its related atmospheric circulation features during the 1991 summer. *Climate Dyn.*, **27**, 815–830, https://doi.org/10.1007/s00382-006-0164-2.

Mao, J. Y., Z. Sun, and G. X. Wu, 2010: 20–50-day oscillation of summer Yangtze rainfall in response to intraseasonal variations in the subtropical high over the western North Pacific and South China Sea. *Climate Dyn.*, **34**, 747–761, https://doi.org/10.1007/s00382-009-0628-2.

Murakami, T., 1980: Empirical orthogonal function analysis of satellite-observed outgoing longwave radiation during summer. *Mon. Wea. Rev.*, **108**, 205–222, https://doi.org/10.1175/1520-0493(1980)108<0205:EOFAOS>2.0.CO;2.

Park, H.-S., B. R. Lintner, W. R. Boos, and K.-H. Seo, 2015: The effect of midlatitude transient eddies on monsoonal southerlies over eastern China. *J. Climate*, **28**, 8450–8465, https://doi.org/10.1175/JCLI-D-15-0133.1.

Ren, P. F., H.-L. Ren, J.-X. Fu, J. Wu, and L. M. Du, 2018: Impact of boreal summer intraseasonal oscillation on rainfall extremes in Southeastern China and its predictability in CFSv2. *J. Geophys. Res.*, **123**, 4423–4442, https://doi.org/10.1029/2017JD028043.

Sampe, T., and S.-P. Xie, 2010: Large-scale dynamics of the Meiyu-baiu rainband: Environmental forcing by the westerly jet. *J. Climate*, **23**, 113–134, https://doi.org/10.1175/2009JCLI3128.1.

Su, Q., R. Y. Lu, and C. F. Li, 2014: Large-scale circulation anomalies associated with interannual variation in monthly rainfall over South China from May to August. *Adv. Atmos. Sci.*, **31**, 273–282, https://doi.org/10.1007/s00376-013-3051-x.

Sun, X. G., G. X. Jiang, X. J. Ren, and X.-Q. Yang, 2016: Role of intraseasonal oscillation in the persistent extreme precipitation over the Yangtze River Basin during June 1998. *J. Geophys. Res.*, **121**, 10 453–10 469, https://doi.org/10.1002/2016JD025077.

Tao, S.-Y., and L. X. Chen, 1987: A review of recent research on the East Asian summer monsoon in China. *Monsoon Meteorology*, C.-P. Chang and T. N. Krishnamurti, Eds., Oxford University Press, 60–92.

Vitart, F., and Coauthors, 2017: The subseasonal to seasonal (S2S) prediction project database. *Bull. Amer. Meteor. Soc.*, **98**, 163–173, https://doi.org/10.1175/BAMS-D-16-0017.1.

Waliser, D. E., K. M. Lau, W. Stern, and C. Jones, 2003: Potential predictability of the Madden–Julian oscillation. *Bull. Amer. Meteor. Soc.*, **84**, 33–50, https://doi.org/10.1175/BAMS-84-1-33.

Wang, B., J. Liu, J. Yang, T. J. Zhou, and Z. W. Wu, 2009: Distinct principal modes of early and late summer rainfall anomalies in East Asia. *J. Climate*, **22**, 3864–3875, https://doi.org/10.1175/2009JCLI2850.1.

Wang, D. H., R. D. Xia, and Y. Liu, 2011: A preliminary study of the flood causing rainstorm during the first rainy season in South China in 2008. *Acta Meteorologica Sinica*, **69**, 137–148, https://doi.org/10.11676/qxxb2011.012. (in Chinese with English abstract)

Wang, S. G., A. H. Sobel, M. K. Tippett, and F. Vitart, 2019: Prediction and predictability of tropical intraseasonal convection: Seasonal dependence and the Maritime Continent prediction barrier. *Climate Dyn.*, **52**, 6015–6031, https://doi.org/10.1007/s00382-018-4492-9.

Wang, S. X., H. C. Zuo, S. M. Zhao, J. K. Zhang, and S. Lu, 2018a: How East Asian westerly jet's meridional position affects the summer rainfall in Yangtze-Huaihe River Valley? *Climate Dyn.*, **51**, 4109–4121, https://doi.org/10.1007/s00382-017-3591-3.

Wang, T. Y., X.-Q. Yang, J. B. Fang, X. G. Sun, and X. J. Ren, 2018b: Role of air–sea interaction in the 30–60-day boreal summer intraseasonal oscillation over the western North Pacific. *J. Climate*, **31**, 1653–1680, https://doi.org/10.1175/JCLI-D-17-0109.1.

Webster, P. J., V. O. Magaña, T. N. Palmer, J. Shukla, R. A. Tomas, M. Yanai, and T. Yasunari, 1998: Monsoons: Processes, predictability, and the prospects for prediction. *J. Geophys. Res.*, **103**, 14 451–14 510, https://doi.org/10.1029/97JC02719.

Wheeler, M. C., and H. H. Hendon, 2004: An all-season real-time multivariate MJO index: Development of an index for monitoring and prediction. *Mon. Wea. Rev.*, **132**, 1917–1932, https://doi.org/10.1175/1520-0493(2004)132<1917:AARMMI>2.0.CO;2.

Wu, J., and X. J. Gao, 2013: A gridded daily observation dataset over China region and comparison with the other datasets. *Chin. J. Geophys.*, **56**, 1102–1111, https://doi.org/10.6038/cjg20130406. (in Chinese with English abstract)

Yang, J., B. Wang, B. Wang, and Q. Bao, 2010: Biweekly and

21–30-day variations of the subtropical summer monsoon rainfall over the lower reach of the Yangtze River basin. *J. Climate*, **23**, 1146–1159, https://doi.org/10.1175/2009JCLI3005.1.

Yasunari, T., 1979: Cloudiness fluctuations associated with the northern hemisphere summer monsoon. *J. Meteor. Soc. Japan*, **57**, 227–242, https://doi.org/10.2151/jmsj1965.57.3_227.

Yasunari, T., 1980: A quasi-stationary appearance of 30 to 40 day period in the cloudiness fluctuations during the summer monsoon over India. *J. Meteor. Soc. Japan*, **58**, 225–229, https://doi.org/10.2151/jmsj1965.58.3_225.

Yuan, C. X., J. Q. Liu, J.-J. Luo, and Z. Y. Guan, 2019: Influences of tropical Indian and Pacific Oceans on the interannual variations of precipitation in the early and late rainy seasons in South China. *J. Climate*, **32**, 3681–3694, https://doi.org/10.1175/JCLI-D-18-0588.1.

Zhang, L. N., B. Z. Wang, and Q. C. Zeng, 2009: Impact of the Madden–Julian oscillation on summer rainfall in southeast China. *J. Climate*, **22**, 201–216, https://doi.org/10.1175/2008JCLI1959.1.

Zhu, C. W., T. Nakazawa, J. P. Li, and L. X. Chen, 2003: The 30–60 day intraseasonal oscillation over the western North Pacific Ocean and its impacts on summer flooding in China during 1998. *Geophys. Res. Lett.*, **30**, 1952, https://doi.org/10.1029/2003GL017817.

Zwiers, F. W., and H. von Storch, 1995: Taking serial correlation into account in tests of the mean. *J. Climate*, **8**, 336–351, https://doi.org/10.1175/1520-0442(1995)008<0336:TSCIAI>2.0.CO;2.